

Interferometric Residual Noise Measurement System

Buabthong, Pakpoom (buabtho2@illinois.edu)

Berenc, Tim (berenc@aps.anl.gov)

Abstract

The low-level radio frequency(rf) control system for the Short-Pulse X-ray project at Argonne requires exceptional precision for differential phase regulation. A phase noise measurement system with a very low noise floor is desired to evaluate the performance of the control system. This paper presents a prototype of an interferometric residual phase noise measurement system operating at 2.815 GHz. The system is an improvement over the previous traditional saturated mixer based system including carrier suppression before detection to overcome dynamic range issues. By using suppression followed by rf amplification, the sensitivity of the interferometric system is increased to 15.6 V/rad compared to 0.3 V/rad for the saturated mixer system, a 32 dB improvement. The experimental result shows a phase noise level of -145 dBrad²/Hz at a 1 Hz offset from the carrier, a 10 dB improvement. In other ranges a 10 to 15 dB improvement is seen. A white noise floor of -175 dBrad²/Hz was obtained with the interferometric system, compared to -170 dBrad²/Hz the the saturated mixer system. Measurements of various contributions to the system reveal that it is the rf amplifier which limits the white noise floor, while the carrier suppression section limits the 1/f and lower frequency noise especially due to microphonics.

1 Introduction

In the Short-Pulse X-ray (SPX) project at Argonne, the stability of the differential phase noise between the radio frequency (rf) cavities plays a crucial role in the performance of the system. The low-level rf (LLRF) control system has to be extremely precise. To measure the performance of the control system, a noise measurement system with a sufficiently low noise floor is needed.

In polar coordinates, the noise of an rf carrier can be represented as amplitude modulation (AM) and phase modulation (PM). Let $\alpha(t)$ and $\varphi(t)$ be amplitude and phase noise. Then, the carrier with noise can be represented as

$$v(t) = V_0(1 + \alpha(t))\cos(\omega_0 t + \varphi(t)) \quad (1)$$

The carrier with noise can also be expressed in Cartesian coordinates as

$$v(t) = V_0\cos(\omega_0 t) + n_I\cos(\omega_0 t) - n_Q\sin(\omega_0 t) \quad (2)$$

In the case when amplitude and phase noise are very small ($\alpha(t), \varphi(t) \ll 1$), Eq.(1) can be well

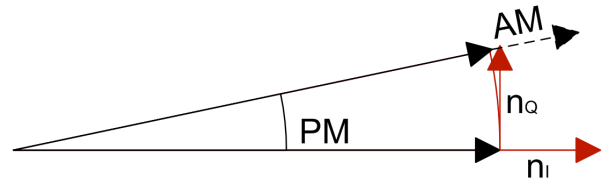


Figure 1: Phasor representation of noise.

approximated as

$$v(t) = V_0\cos(\omega_0 t) + V_0\alpha(t)\cos(\omega_0 t) - V_0\varphi(t)\sin(\omega_0 t) \quad (3)$$

Thus the polar and Cartesian coordinates can be related as

$$n_I(t) = \alpha(t) \cdot V_0 \quad (4)$$

$$n_Q(t) = \varphi(t) \cdot V_0 \quad (5)$$

Since the carrier can be written as $V_0\cos(\omega_0 t) = \text{Re}\{V_0e^{j\omega_0 t}\}$, Eq.(2) can be written in terms of phasors rotating with the

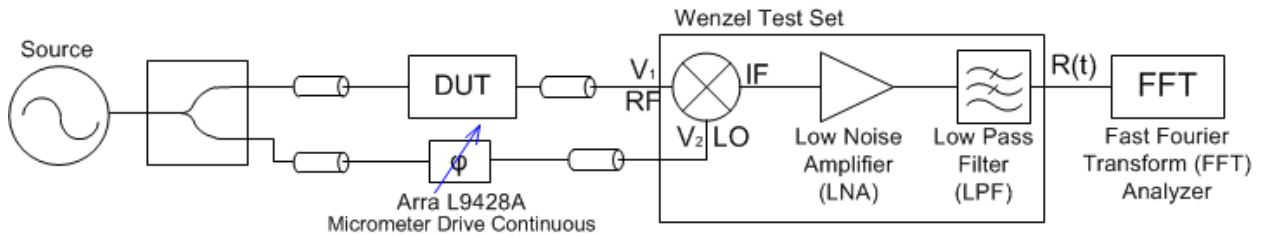


Figure 2: Scheme of the saturated mixer set-up for phase noise measurement.

carrier frequency as

$$v(t) = \text{Re}\{(V_0 + V_0\alpha(t) + iV_0\varphi(t))e^{j\omega_0 t}\} \quad (6)$$

This allows one to look at the phasor within the rotating frame (See Fig.1).

Since the SPX phase specification is a differential specification and is much lower than the amplitude specification, this paper focuses on residual phase noise.

The simplest approach to measure phase noise uses the technique of a saturated mixer, which mixes a device under test's (DUT) output with a 90° phase shifted version of the common source signal as depicted in Fig.2. The noise floor of the saturated mixer system was found to be limited by the noise floor of the baseband low noise amplifier (LNA), the mixer, and cable vibrations. The interferometer on the other hand overcomes an inherent dynamic range issue in the saturated mixer system by allowing the noise around the carrier to be amplified before detection in the mixer. The result is an increase in the sensitivity of the system, hence overcoming limitations of the baseband section.

The measurement system represented here is designed for S-band operating at 2.815GHz . It was built in an unshielded laboratory, located at the Advanced Photon Source of Argonne National Laboratory. Therefore, disturbance from conducted power line interference from accelerator operations, other nearby lab spaces, electromagnetic interference, and mechanical vibrations are expected in the result.

2 Noise Measurement Methods

2.1 Traditional Saturated Mixer

To measure the noise added to the carrier by the device under test (DUT), a mixer is used as the detector of the product of the two signals at the RF and Local Oscillator (LO) ports of Fig.2. Carefully adjusting the carrier's power to saturate the mixer makes the mixer insensitive to amplitude modulation of the carrier [1]. With the phase difference between the RF and LO ports set to 90° , the mixer ideally detects only phase modulation. From Fig.2, the intermediate frequency (IF) output of the mixer becomes a baseband signal when $v_{LO}(t) = V_2 \sin(\omega_0 t)$ and $v_{RF}(t) = V_1 \cos(\omega_0 t + \varphi(t))$ and is given as

$$\begin{aligned} v_{IF}(t) &= V_1 \cos(\omega_0 t + \varphi(t)) \cdot V_2 \sin(\omega_0 t) \quad (7) \\ &= V_1 V_2 \left[-\frac{\sin(\varphi(t))}{2} + \sin(2\omega_0 t) \cos(\varphi(t)) \right. \\ &\quad \left. + \frac{\cos(2\omega_0 t) \sin(\varphi(t))}{2} \right] \quad (8) \end{aligned}$$

Assuming small phase noise such that $\sin(\varphi(t)) \approx 0$ and $\cos(\varphi(t)) \approx 1$, Eq.(8) can be well approximated as

$$v_{IF}(t) = V_1 V_2 \left[\frac{\varphi(t)}{2} + \sin(2\omega_0 t) \right] \quad (9)$$

The low-pass filter (LPF) then eliminates the double frequency term. The noise at the output to the Fast Fourier Transform (FFT) analyzer is then simply

$$R(t) = -V_1 V_2 \frac{\varphi(t)}{2} \quad (10)$$

$$= k_\varphi \varphi(t) \quad (11)$$

where k_φ is a scaling factor [V/rad] converting the readout of the FFT analyzer from dBV^2/Hz

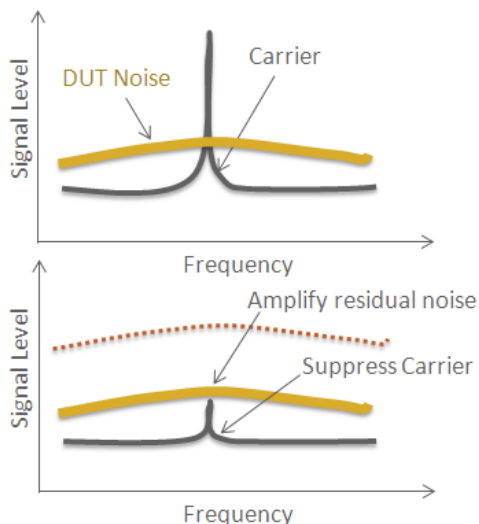


Figure 3: Principle of the Interferometer Technique.

to dBrad^2/Hz . Since the mixer is saturated, amplitude fluctuations of V_1 and V_2 are ideally suppressed.

2.2 Interferometer

In an attempt to better detect the residual noise and obtain a lower noise floor, carrier suppression is introduced in the interferometric technique. From Fig.3, ideally the carrier and its inherent noise from the source is suppressed, leaving behind the residual noise from the DUT which can then be amplified before detection in the mixer. This overcomes dynamic range issues if one was to try to amplify the DUT's noise in the presence of the large carrier. With the carrier suppressed, only the noise is amplified. This greatly increases the sensitivity of the measurement system. As shown in Fig.4, the carrier-suppressed signal goes into the bandpass filter which eliminates out-of-band noise that could saturate the amplifier. and cause a higher noise floor [2]. The RF amplifier then amplifies the residual noise and overcomes the noise floor of the mixer and low-noise amplifier.

While the interferometer-based system exhibits a lower noise floor, the result depends heavily on the stability of the system. Any

subtle mechanical perturbation can cause an increase in the noise floor level. Hence, the set-up of an interferometric system should be properly mounted.

3 Experimental Results

3.1 Saturated Mixer Results

Although developing a phase noise measurement system to evaluate the performance of the SPX's LLRF control system is the main motivation for this project, this experiment only covers the measurement of the system's noise floor. This is done using the set-up for a saturated mixer according the scheme in Fig.2, but now with a simple piece of coax cable replacing the DUT.

3.1.1 Calibration, Scaling Factor

In order to make a saturated mixer system measure phase noise, the carrier's phase at the LO and IF ports of the mixer have to be 90° out of phase. The length difference of the two paths can be approximated with the assumption that the signal is traveling in the cable at 0.8 times the speed of light. In this experiment, the frequency of the carrier is 2.815GHz. Therefore, the wavelength (λ) is approximately $\frac{v}{f} = \frac{0.8 \cdot (2.99 \cdot 10^8)}{2.815 \cdot 10^9} = 0.0850m$. Therefore, for 90° phase difference, the length difference has to be about 2.13 cm. After setting the cable with a rough calculation, the phase difference can be precisely adjusted using the manual phase shifter while monitoring the voltage at the output of the mixer. According to Eq.8, we can adjust the phase shifter until the nominal DC voltage at the mixer output reaches zero.

The FFT analyzer displays a power spectral density measurement in units of $[\text{V}^2/\text{Hz}]$. Thus a scaling factor is needed to convert voltage units into phase units. To measure the scaling factor in a saturated mixer system, the ratio of phase change to voltage change is needed. Since the system includes the adjustable phase shifter, an intermediate scaling is needed relating the phase shifter at 2.815 GHz per unit turn of the phase shifter. The ratio of V/rad can then be deter-

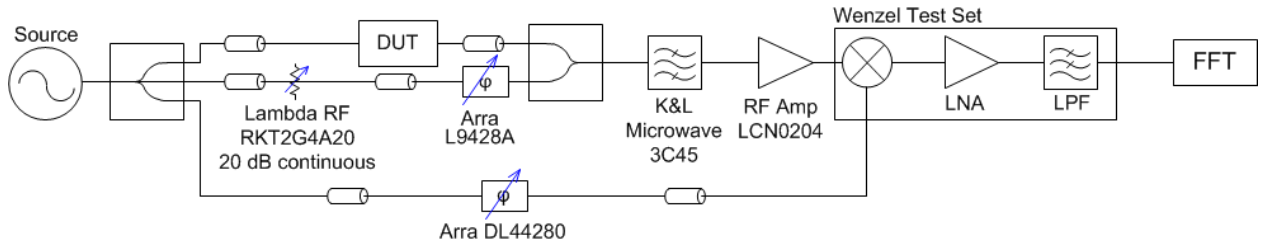


Figure 4: Scheme of an interferometric noise measurement system.

mined by measuring the change in voltage at the output of the mixer for a given adjustment of the phase shifter micrometer drive. The phase noise in dBrad^2/Hz can then be calculated by subtracting the scaling factor in dB from the raw data reported as dBV^2/Hz from the FFT analyzer.

For this experiment, a network analyzer showed that the phase shifter (ARRA L9428A) changes the phase at 2.815GHz by 0.3 rad per unit ($1/10$ inch). The corresponding DC voltage at the output of the mixer is 115 mV. Hence the mixer scaling is calculated as 0.385 V/rad. The LNA in the Wenzel Test Set has a gain of 60dB or $10^{\frac{60}{20}} = 1000$ in voltage. Hence, the overall scaling factor is

$$k_\varphi = \frac{1000 \cdot 0.1151}{0.2988} \quad (12)$$

$$= 385 \text{ V/rad} \quad (13)$$

Thus, the phase noise in dBrad^2/Hz can be calculated by subtracting $(60\text{dB} + 20 \log_{10}(k_\varphi)) = 51.71$ dB from the raw dBV^2/Hz FFT data.

3.1.2 Low Noise Amplifier

A low-noise amplifier is inserted after the mixer to amplify the residual noise of DUT (or, in this experiment, the noise floor of the saturated mixer set-up). If the noise floor of the system is lower than that of the FFT analyzer, the measured noise floor will be the noise floor of FFT analyzer, not the measurement system.

When two noise sources are added, the higher noise source dominates. If there are two noise sources at the level of $-a$ dB and $-b$ dB where

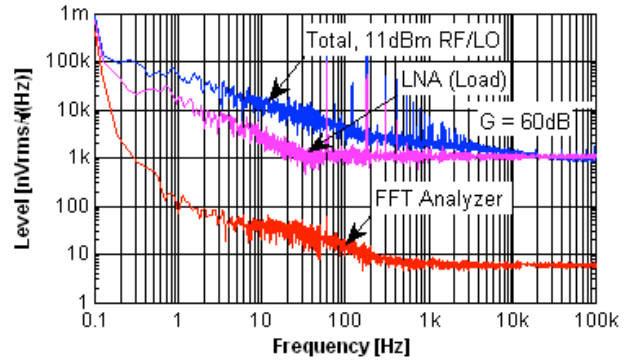


Figure 5: Noise Referred to the Output of the LNA.

$-a > -b$ (b is Δ dBV lower) the power of the combined noise adds as

$$10 \log(P_a + P_b) = 10 \log(10^{-\frac{a}{10}} + 10^{-\frac{b}{10}}) \quad (14)$$

$$= 10 \log(10^{-\frac{a}{10}}) + 10 \log(1 + 10^{-\frac{\Delta}{10}}) \quad (15)$$

Therefore, a Δ dBV lower noise contributes $10 \log(1 + 10^{-\frac{\Delta}{10}})$ dBV to the overall noise.

To confirm this calculation, the noise floor of the system was made with and without LNA. First, the noise level from the LNA at 50 Hz was found to be lower than the noise floor by 10 dBV^2/Hz . Next, the total system's noise floor measured with the amplifier is 132.5 dBV^2/Hz and 132.05 dBV^2/Hz without the LNA. This shows the contribution of 0.45 dBV^2/Hz from a 10 dBV^2/Hz lower noise, which is close to $10 \log(1 + 10^{-\frac{10}{10}}) = 0.41$ dBV^2/Hz from the prediction.

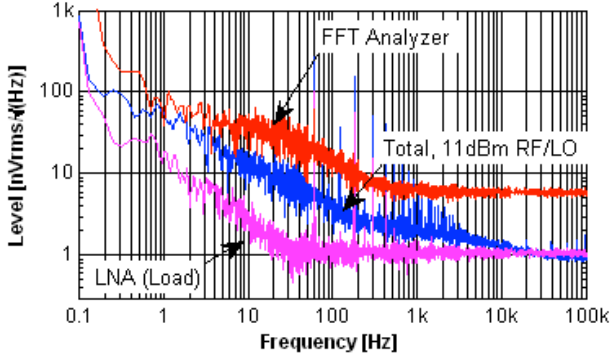


Figure 6: Noise Referred to the Input (RTI) of the LNA Compared to the Noise Floor of the FFT Analyzer.

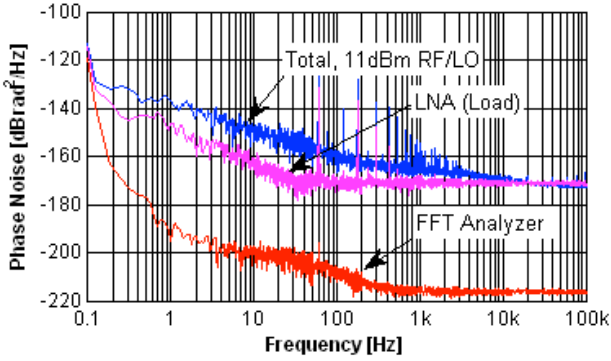


Figure 7: Contributions to Test Set Noise Floor.

3.1.3 System Noise Floor

First, in order to saturate the mixer, the RF generator is carefully adjusted until the power level at the input of the mixer is 11 dBm.

Figure 5 shows raw measurements at the FFT analyzer for (1) the total noise floor of the measurement system, (2) the LNA with a 50Ω load at its input, (3) FFT analyzer alone with a 50Ω input termination. The actual noise floor of the measurement system and the LNA as referred to the input of the LNA can be obtained by subtracting the amplifier gain of 60 dB, resulting in Fig.6. This shows how the system can overcome the noise floor of the FFT analyzer.

The total noise floor of the system referred to the input of the LNA is only $1\text{-}2 \text{ nV}_{rms}/\sqrt{\text{Hz}}$, while the noise floor of the FFT analyzer is around $5 \text{ nV}_{rms}/\sqrt{\text{Hz}}$. Without the LNA, the noise floor of the system would be limited by the

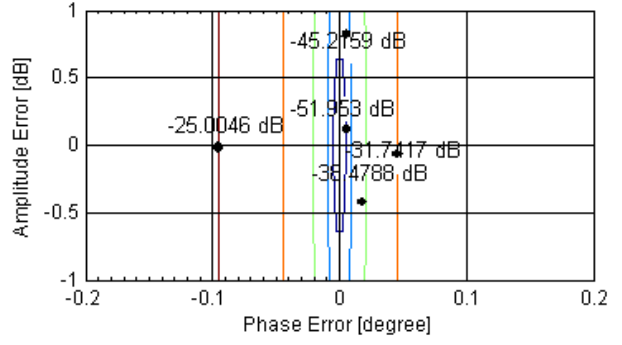


Figure 8: Carrier Suppression with Amplitude and Phase Error.

FFT analyzer's noise floor.

Using the scaling factor (k_φ), the actual phase noise floor can be obtained. Referring to Fig.7, the white noise floor of the total system is $-170 \text{ dBrad}^2/\text{Hz}$, and the flicker noise at 1Hz offset from the carrier is $-140 \text{ dBrad}^2/\text{Hz}$. The white noise from the amplifier is about the same level $-170 \text{ dBrad}^2/\text{Hz}$. While its flicker noise at 1 Hz offset is about 10dB lower at $-150 \text{ dBrad}^2/\text{Hz}$. Lastly, the white noise floor contribution of the FFT analyzer is effectively $-220 \text{ dBrad}^2/\text{Hz}$.

From Eq.(15), the contribution of the FFT analyzer to the total noise floor is only $10 \log(1 + 10^{-\frac{50}{10}}) = 4.34 \cdot 10^{-5} \text{ dB}$, which is negligible.

Although the noise floor of the system can overcome the FFT analyzer's noise floor by getting amplified by LNA, a lower noise floor can be achieved by suppress the carrier and amplify the noise sideband before detection.

3.2 Interferometer Result

To minimize mechanical vibrations of the system, shown in Fig.10, the prototype is mounted to a metal plate; All the semi-rigid cables are secured by adhesive tape.

3.2.1 Carrier Suppression

To suppress the carrier before the amplifier, manual attenuators and phase shifters are used to properly orient the signal at (a), (b), (e) in Fig.9. Both attenuation and phase has to be carefully adjusted to achieve maximum suppression. From Fig.8, small amplitude error and

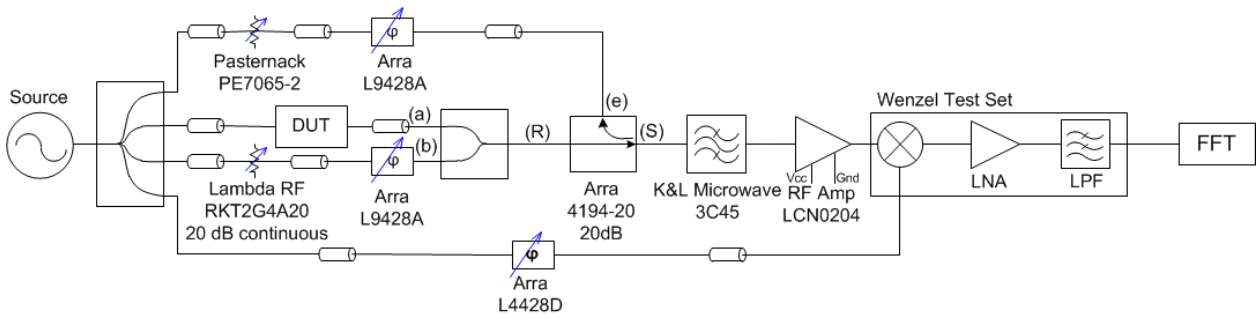


Figure 9: Scheme of the interferometric noise measurement system with fine adjust.

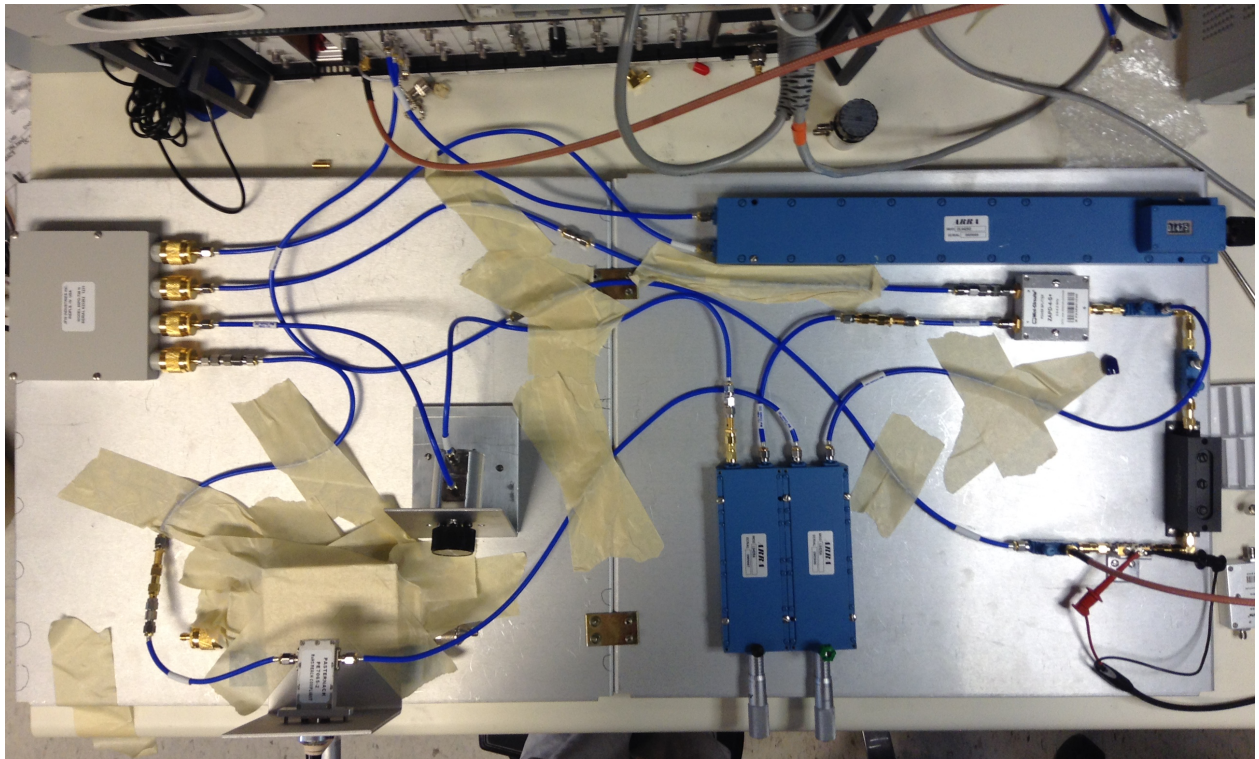


Figure 10: Interferometric System's Prototype.

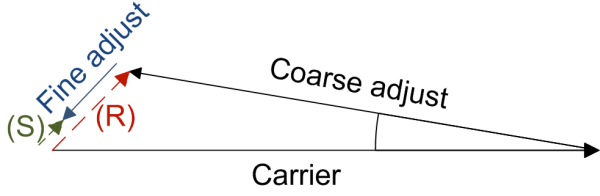


Figure 11: Vector Representation of Coarse and Fine Adjust.

phase error can introduce a great loss in carrier suppression.

3.2.2 Coarse adjust

In the coarse adjust (path (b) in Fig.9), a by-step attenuator is used because it is less sensitive to mechanical fluctuations of contacts [3]. Neglecting accuracy of the attenuator, using a 0.1 dB step attenuator will lead to at most a 0.05 dB error in amplitude difference. The signals at (a) and (b) could thus be considered to be related as

$$20 \log\left(\frac{b}{a}\right) = -0.05 \quad (16)$$

$$b = a(10^{-\frac{0.05}{20}}) \quad (17)$$

Neglecting any phase errors, when the signals are recombined, this would result in

$$R = a - c \quad (18)$$

$$= a(1 - 10^{-\frac{0.05}{20}}) \quad (19)$$

$$= 0.0057a \quad (20)$$

This corresponds to a suppression of

$$20 \log\left(\frac{a}{R}\right) = 20 \log(1/0.0057) \quad (21)$$

$$= 44.82dB \quad (22)$$

If one is lucky in adjusting (b), better suppression can be achieved. However we found that typical coarse adjustment rarely gave better than 50 dB suppression and usually less than this.

3.2.3 Fine Adjust

A carrier suppression of 45 dB could still cause the rf amplifier to saturate either from the cw

output carrier approaching the 1 dB compression point and/or instantaneously from the carrier plus peak noise. It also allows the rf amplifier to cause flicker noise around the carrier which can limit the low frequency noise floor of the measurement system [4]. Therefore, a fine adjust is incorporated. From Fig.11, the fine adjust signal is much smaller compared to the coarse adjust signal. Ideally, it cancels the residual carrier left from the coarse adjust. With a 20 dB directional coupler (ARRA 4194-20), the fine adjust controls a very small signal to cancel the carrier. As a result, the path is less sensitive to mechanical fluctuations of the attenuator contacts. Therefore, a continuous attenuator can be used in this path. The fine adjust should ideally have the same magnitude and opposite phase of the residual vector left from the coarse adjust. A proper amount of fixed attenuation needs to be included, taking into account the directional coupler and nominal variable attenuator setting, in order to get the fine adjust vector within range of the residual vector. As an example of how the fine adjust is desensitized to variable attenuator errors/fluctuations, let the signal in the fine path ideally be $e = R = a(1 - 10^{-\frac{0.05}{20}})$. Then, if a 0.5 dB error is introduced, the combined signal at the output of the directional coupler is

$$S = R - e(1 - 10^{-\frac{0.05}{20}}) \quad (23)$$

$$= a(1 - 10^{-\frac{0.05}{20}}) \quad (24)$$

$$- a(1 - 10^{-\frac{0.05}{20}})(10^{-\frac{0.05}{20}})$$

$$= a(1 - 10^{-\frac{0.05}{20}})^2 \quad (25)$$

$$= (3.29 \cdot 10^{-5})a \quad (26)$$

which, corresponds to a suppression of

$$20 \log\left(\frac{a}{S}\right) = 20 \log(1/3.29 \cdot 10^{-5}) \quad (27)$$

$$= 89.64dB \quad (28)$$

Unlike the saturated mixer system, a voltage measurement at the output of the mixer cannot be used to calibrate the LO in an interferometer system because the carrier at the RF port has already been suppressed. From Fig.12, the measurement plane has to match the DUT signal. If

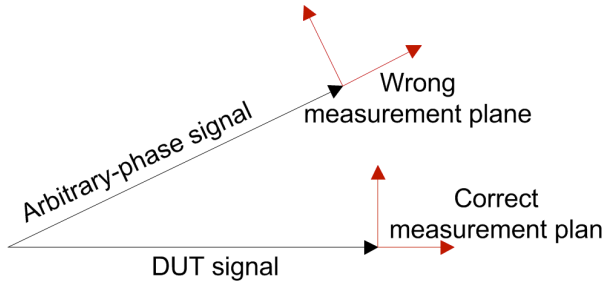


Figure 12: Principle of the LO Calibration.

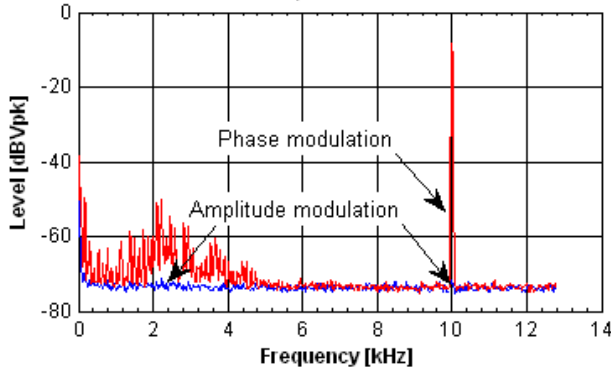


Figure 13: LO Adjust Using Voltage Controlled Attenuator (VCA) and Voltage Controlled Phase Shifter (VCPS).

the two do not match, both phase and amplitude modulation of the DUT would get projected onto the quadrature component of the measurement plane.

Previous literature suggests replacing the DUT with a phase shifter, adjusting the LO, and changing back to the DUT [4]. However, when switching the DUT and phase shifter, the phase relationship between the LO and the DUT is not necessarily constant. To make sure that the measurement plane is in the same plane as that of the LO, the LO and DUT path should be left undisturbed for the entire period of calibration and experiment.

As a result, a voltage controlled attenuator (VCA) is inserted into the nulling arm to indicate the phase of the carrier path. First, maximum carrier suppression is needed to confirm that the resultant signal is collinear with the DUT signal. Then, by driving the VCA with a specific frequency, the amplitude modulation appears in

the power spectral density at the modulation frequency. Adjusting the LO phase to detect phase noise would make the system insensitive to any amplitude modulation, including the one from the VCA. Therefore, by adjusting the LO phase until the detected signal at the VCA's modulation frequency is minimized, the measurement plane coincides with the DUT's signal plane. After removing the VCA, the carrier suppression can be readjusted, without any perturbation to LO-DUT phase relationship.

Another way to adjust the LO path is to use a Voltage Controlled Phase Shifter (VCPS) instead of a VCA and adjust for the maximum value in the power spectral density. Fig.13 shows a comparison between using a VCA and a VCPS to adjust the LO. Unlike using a VCA, finding the maximum of the modulation is very difficult. Tuning to the maximum of a quadrature component (from a VCPS' modulation) requires working at the peak of a sinusoidal function (From Eq.(2)), while using a VCA allows us to adjust the zero crossing region of a sinusoid. Consequently, using amplitude modulation is more practical.

3.2.4 Scaling factor

To calculate the scaling factor of an interferometric system, an additional RF generator is needed to provide a secondary source as a sideband signal, the V/rad ratio can be found by comparing the amplitude of the sideband to the amplitude of the unsuppressed carrier. Since the voltage is proportional to the square root of the power, the amplitudes of the carrier and the sideband are proportional to $\sqrt{P_0}$ and $\sqrt{P_s}$. Hence, the quadrature modulation associated with the sideband can be written as $n_Q(t) = \sqrt{P_s} \sin(\Delta ft)$. The relationship between quadrature component and phase modulation for a small noise from Equation (5), can be rewritten as

$$\varphi(t) = \frac{n_Q}{V_0} \quad (29)$$

$$= \sqrt{\frac{P_s}{P_0}} \sin(\Delta ft) \quad (30)$$

From Equation(11), the scaling factor can be calculated using the peak voltage read from the FFT analyzer as

$$k_\varphi = \frac{V_{FFT}}{\varphi(t)} \quad (31)$$

$$= \frac{V_{pk} \sin(\Delta ft)}{\sqrt{P_s} / \sqrt{P_0} \sin(\Delta ft)} \quad (32)$$

$$= \sqrt{\frac{P_0}{P_s}} \cdot V_{pk} \quad (33)$$

It is also important to note that while the power level of the carrier can be high (8.32 dBm in this experiment), the level of the RF Generator that produces the sideband has to be very low to keep the system from saturating (-90 dBm). In this experiment, we measured the power of the carrier and sideband to be 8.32 dBm and -93.2 dBm respectively with a peak voltage from the FFT analyzer of 131.2 mV. Hence the mixer scaling is calculated as 15.63 V/rad. Similar to the saturated mixer system, the LNA has a gain of 60dB or $10^{\frac{60}{20}} = 1000$ in voltage. Consequently, the overall scaling factor of this interferometric system is

$$k_\varphi = \sqrt{\frac{P_0}{P_s}} \cdot V_{pk} \quad (34)$$

$$= \sqrt{\frac{10^{P_0, dB}/10}{10^{P_s, dB}/10}} \cdot V_{pk} \quad (35)$$

$$= \sqrt{\frac{10^{8.32/10}}{10^{-93.2/10}}} \cdot 131.2 \cdot 10^3 \quad (36)$$

$$= 15630 \text{ V/rad} \quad (37)$$

3.2.5 RF Amplifier

The rf amplifier is a crucial component of the system. It should provide high enough gain to achieve good sensitivity while having a low noise figure to achieve a low white noise floor for the system. It should also have low flicker noise to deal with imperfect carrier suppression. The amplifier chosen here was a Miteq LCN0204.

3.2.6 Contributions to the Noise Floor

From Fig.14, the noise floor of the interferometric system is lower with a white noise floor of -

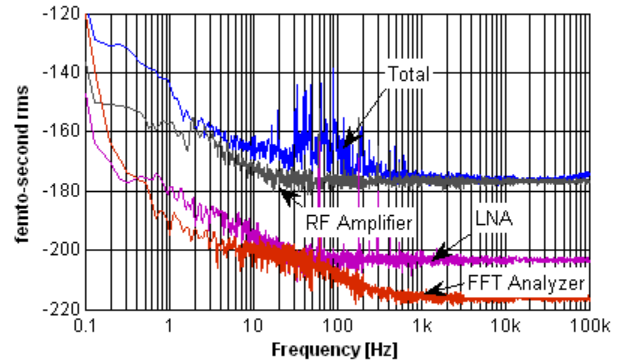


Figure 14: Contributions to Test Set Noise Floor.

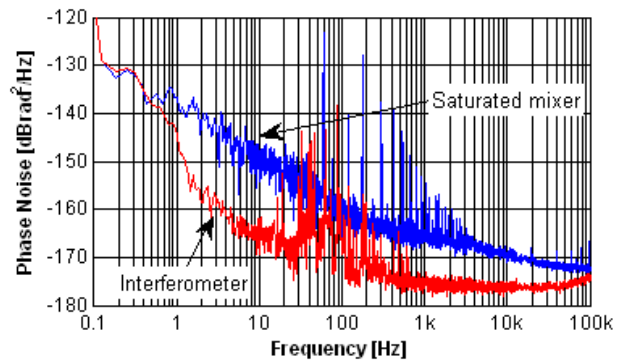


Figure 15: Phase Noise from Saturated Mixer and Interferometric System.

175 dBrad²/Hz, and ~ -145 dBrad²/Hz at a 1Hz offset.

When terminating the input of the RF amplifier, the measured noise floor indicates the noise floor from the amplifier and baseband electronics. Thus, any additional noise is due to the interferometer stability. Also, imperfect carrier suppression can cause the amplifier to flicker.

Fig.14 shows that the rf amplifier's white noise floor limits the noise floor of the system. However, both LNA and FFT analyzer's noise floor are lower than the noise floor of the system.

4 Conclusion

From the experiment, the phase noise level of the interferometer, shown in Fig.15, exhibits the improvement over the saturated mixer. The white noise floor in the interferometric system is lower by 5 dBrad²/Hz, and around 10-15 dBrad²/Hz

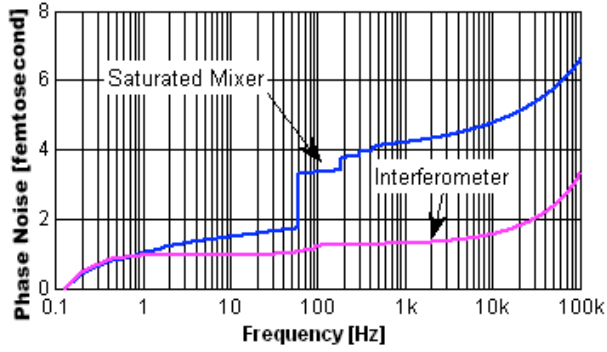


Figure 16: Phase Noise from Saturated Mixer and Interferometric System.

from 1Hz - 1kHz offset from the carrier. Also, Fig.16 shows that the cumulative integral phase noise from the interferometric system is much lower than that from the saturated mixer system. Even though the cumulative integrals for both systems are at the same level from 0.1Hz - 1Hz, the interferometer exhibits 0.02 femtosecond

By carefully suppressing the carrier and inserting an rf amplifier before the mixer, we can greatly increase the sensitivity and overcome the noise floor limitations of the baseband electronics. However, the limitations are then pushed into the carrier suppression and rf sections. Regardless, the results show a substantial improvement.

The sensitivity of the interferometric system is 15.63 V/rad compared to 0.385 V/rad for the saturated mixer system. This is a factor of 40.59 times or 32.17 dB higher. Due to the increased sensitivity and multiple components making up the interferometer section, it is susceptible to perturbations due to mechanical and electromagnetic interference. The sensitivity of an interferometric system increases from 0.3 V/rad (in a saturated mixer system) to 15.63 V/rad. Nevertheless, it leads to a greater dependence on the system's mechanical stability which requires an additional caution when collecting the result.

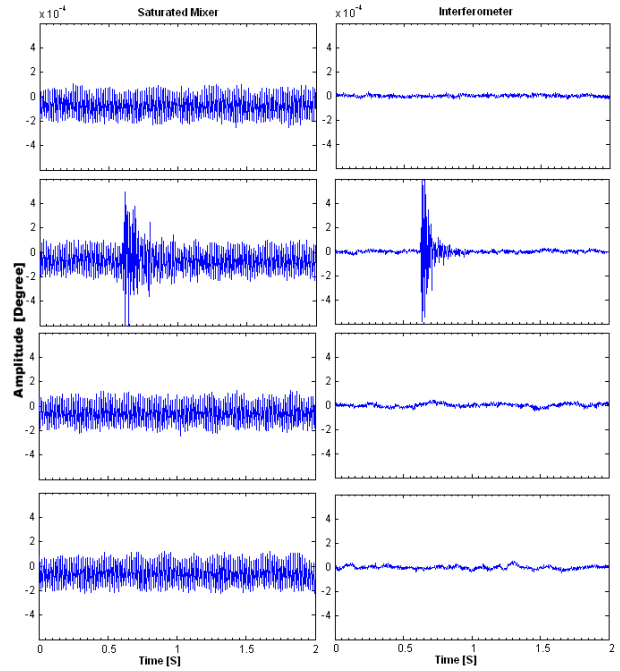


Figure 17: Outputs of FFT Analyzer in a Time Domain. (a) Without any disturbance (b) Knock on the table (c) Walking (d) Waving over the set-up.

5 Future recommendations

Both the saturated mixer and the interferometric system make use of amplifiers. In particular, the interferometric system relies heavily on the RF amplifier while the saturated mixer relies more heavily on the low frequency LNA. Using amplifiers with a sufficiently low noise floor can improve the noise floor of the system.

During the experiment, the main issue we faced was mechanical vibration of the system. Any subtle movement around the experimental area could cause changes in the result, especially in the interferometric system. Plotted on the same scale, Fig.17 shows that the interferometric system is more sensitive to mechanical vibration probably due to the increased number of components compared to the saturated mixer system. When knocking on the table, even though both saturated mixer and interferometer show a pulse in their time domain data, the pulse in the interferometric system appeared higher. Furthermore, when walking or waving a hand over the

set-up, the saturated mixer system exhibits no difference than its normal state, while the interferometric system was very sensitive to these actions (1) because of the increased sensitivity of the system itself and (2) because any electromagnetic interference disturbs the carrier suppression and shows up as noise.

For an interferometric system, these mechanical vibrations play an important role in the system's performance. Therefore, in the future experiment, mounting the system on an isolated optical table and using better shielded coaxial cables could provide more mechanical stability and better performance.

References

- [1] K. H. Sann, "The Measurement of Near-Carrier Noise in Microwave Amplifiers," *IEEE Trans. Microw. Theory Techs.*, no. 9, pp. 761-766, 1968.
- [2] R. Boudot, E. Rubiola, "Phase Noise in RF and Microwave Amplifiers," arXiv:1001.2047v1 [physics.ins-det], Jan. 2010, submitted to *IEEE Trans. MTT*.
- [3] E. Rubiola, V. Giordano, "A Low-Flicker Scheme for the Real-Time Measurement of Phase Noise," *Proc. 2001 Freq. Control Symp.*, pp. 138-143, 2001.
- [4] E. Rubiola, V. Giordano, "Advanced Interferometric Phase and Amplitude Noise Measurement," *Rev. Sci. Instrum.*, vol. 73 no.6 pp. 2445-2457, 2002.